To be published in Applied Optics:

Title:	Reducing the impact of source brightness fluctuations on spectra obtained by FTS
Authors:	Gretchen Keppel-Aleks, Geoffrey Toon, Paul Wennberg, and Nicholas Deutscher
Accepted:	22 March 2007
Posted:	23 March 2007
Doc. ID:	79475

Reducing the impact of source brightness fluctuations on spectra obtained by FTS

Gretchen Keppel-Aleks[1], Geoffrey C. Toon[2], Paul O. Wennberg[1], Nicholas M. Deutscher[3]

[1] *California Institute of Technology*

1200 E California Blvd., Pasadena CA 91125

[2] *NASA Jet Propulsion Laboratory, California Institute of Technology*

4800 Oak Grove Dr., Pasadena CA 91109

[3] *University of Wollongong*

Wollongong NSW 2522 Australia

gka@gps.caltech.edu

We present a method to reduce the impact of source brightness fluctuations (SBF) on spectra recorded by Fourier Transform Spectrometry (FTS). Interferograms are recorded without AC coupling of the detector signal (DC mode). The SBF are determined by low-pass filtering of the DC interferograms, which are then re-weighted by the low-pass, smoothed signal. Atmospheric solar absorption interferograms recorded in DC mode have been processed with and without this technique, and we demonstrate its efficacy in producing more consistent retrievals of atmospheric composition. We show that the re-weighting algorithm improves retrievals from interferograms subject to both gray and non-gray intensity fluctuations, making the algorithm applicable to atmospheric data contaminated by significant amounts of aerosol or cloud cover.

OCIS codes: 010.1280, 070.6020

1. Introduction

Traditionally, a high-pass analog filter has been used in Fourier Transform Spectrometry (FTS) signal chains. This method, called AC recording, has been preferred over DC recording (in which the detector signal is not high-pass filtered prior to digitization) for two reasons. First, most ADCs encompass positive and negative values, so recentering the interferogram at zero, as is done in AC recording, enables the

full dynamic range of the ADC to be utilized without the complication of subtracting an electrical offset. Second, AC recording facilitates gain switching, necessary in high-resolution FTS to resolve the interferogram at both high and low optical path difference (OPD). At low OPD - the center burst of the interferogram - the fringes are several orders of magnitude larger in amplitude than those at high OPD. Use of a single gain to record the interferogram requires that the signal be sampled with very large dynamic range (greater than 16 bit resolution), typically in excess of the range available for fast ADCs. Therefore, gain switching during a scan is employed on many high-resolution FTS instruments to avoid saturation of the interferogram at low OPD while amplifying the small fringes at high OPD sufficiently to avoid digitization noise. To accomplish this, the large DC term must be eliminated to center the interferogram at 0 V, consistent with the usual bipolar ADC inputs.

AC recording entails loss of information regarding source brightness fluctuations (SBF) that occur during interferogram acquisition. Since SBF are multiplicative, their effect cannot be removed simply by high-pass filtering; the high frequency interferogram fringes have been amplitude-modulated. Spectrometrists have long recognized that "ratio-recording" reduces the impact of variations in source intensity and have gone to great lengths to implement ratio-recording techniques (e.g. Ahlers et al., 1954).[1] FTS systems are even more sensitive to such variations than are grating spectrometers due to the fact that the low and high resolution information is not acquired simultaneously. Because the zero path difference (ZPD) region of the in-

terferogram sets the continuum level of the resulting spectrum, while the high OPD fringe amplitudes determine the line depths, SBF during sampling of the interferogram affect broad and narrow spectral features differently. Intensity loss at one region of the interferogram can therefore distort the fractional line depths, since SBF lead to multiplicitave modulation of fringe amplitude.

The DC interferogram can be used to correct for SBF, minimizing the errors that such fluctuations introduce into the spectra. By use of an appropriate digital filter, the low frequency variation due to SBF can be separated from the higher frequencies that contain the interferometrically modulated energy. Knowledge of this DC intensity can then be used to correct for slow variations in source intensity as an interferogram is obtained. This is a fundamentally different approach than that of Shao et al., who attempt to identify and reject interferograms affected by SBF.[2]

We present here a method and an algorithm that correct for SBF. DC interferograms are passed through a low-pass filter, and the resulting low-pass signal is used to normalize all regions of the interferogram. In re-weighting the interferogram, the relative line depth to continuum level ratio is corrected as the fringes altered by SBF are normalized. Use of inexpensive high dynamic range delta-sigma ADCs (24 bits) facilitates such a correction. The large dynamic range eliminates the need for gain switching to properly resolve the high OPD regions of the interferogram. A single interferogram can then be recorded in low gain without high-pass filtering. Although not demonstrated here, similar benefits could be derived from a lower resolution ADC

with two output channels: a low gain DC interferogram and a high gain AC interferogram. The low gain, smoothed DC term would be sufficiently resolved to re-weight an interferogram derived from the two channels.

In section 2, we present our methodology for correcting DC interferograms and our re-weighting algorithm. In sections 3 and 4, we discuss the application of the re-weighting algorithm to solar absorption spectrometry and present a comparison between data processed with and without the re-weighting algorithm. Section 5 examines the efficacy of the re-weighting algorithm in processing spectra affected by non-gray SBF. The influence of detector nonideality on the re-weighted interferogram is discussed in section 6.

2. Methods

The algorithm devised to correct for intensity variations is straightforward and had been suggested in the past by Brault (1985).[3] We take a real-to-complex fast Fourier transform of the raw DC interferogram. To the resulting spectrum we apply the spectral filter of Equation 1 which retains frequencies below the cutoff frequency s.

$$F = \begin{cases} \left(\frac{1+cos(\frac{\pi\nu}{s})}{2}\right)^N & \text{if } \nu < \text{s} \\ 0 & \text{if } \nu > \text{s} \end{cases} \tag{1}$$

We choose s=300 cm^{-1} (180 s^{-1}) corresponding to 8% of the low frequency detection limit for the spectra described here, and N=8. The frequency cutoff, s, should be

minimized such that it is smaller than the lowest frequency at which interferometric modulation is measured, while still larger than the characteristic SBF frequency. The parameter N determines the steepness of the filter cutoff. A large difference between the characteristic SBF frequency and the low frequency detection limit allows a wider range of permissible s values, and lowers the sensitivity to choice of N. In instances where the highest SBF frequency and the low frequency detection limit are similar, a higher value of N is desired to increase the filter steepness. We discuss the sensitivity of the data to choice of s in section 6.

We take the inverse Fourier Transform of the low-frequency spectrum that results from Equation 1 using a complex-to-real routine. The resulting low pass-filtered interferogram provides a measure of the SBF at frequencies well below the signal due to interferometric modulation. Ratioing the raw interferogram to this smoothed interferogram yields an interferogram with constant DC level of one, with all regions of the interferogram having a uniform intensity weighting.

$$I_{corr}(x) = \frac{I_{raw}(x)}{I_{smooth}(x)} * I_{smooth}(ZPD) \tag{2}$$

We choose to scale the re-weighted interferogram by the DC level at ZPD, as written in Equation 2, so that each interferogram retains information on the absolute intensity at ZPD, which is helpful in many applications. The corrected interferogram can then be processed using standard interferogram processing routines.

3. Application

SBF affect many spectra obtained by FTS. Remote sensing is particularly susceptible as scene brightness often changes during the acquisition of an interferogram. We illustrate the benefits of the re-weighting algorithm with measurements of infrared solar spectra obtained from the Earth's surface. Ground-based direct solar absorption spectrometry is a common technique used to infer atmospheric composition. High resolution FTS has been used historically by the Network for the Detection of Atmospheric Composition Change (previously called the Network for the Detection of Stratospheric Change).[4] Although using the sun as a source provides excellent signal-to-noise, the source intensity can vary on the timescale of a single scan due to attenuation by clouds and aerosol. Such variability degrades the accuracy and precision of gas amounts retrieved from such spectra.

In our application, we use near infrared solar absorption spectra to obtain total column abundance of atmospheric gases including O_2, CO_2, CO, CH_4, and H_2O.[5] These measurements are obtained at Park Falls, WI and Darwin, Australia, sites affiliated with the Total Carbon Column Observing Network (TCCON).[6] The goal of TCCON is to provide constraints on variability in surface fluxes of CO_2. To accomplish this, it is necessary to obtain precisions in column retrievals better than 0.5%. To meet the required precision without the DC correction, interferograms obtained with high SBF, as determined by a measurement of the total solar intensity on a solar

tracker quadrant sensor, were discarded. Eliminating these spectra greatly reduced the range of atmospheric conditions under which worthwhile observation was possible. Even optically thin clouds crossing the field of view of the instrument rendered the measurements unusable. Incorporation of the DC correction allows many of these otherwise-discarded spectra to be used.

Data are obtained using a Bruker IFS 125HR Fourier Transform Spectrometer. The instrument is optimized for recording in the near infrared, with gold coated optics and a CaF_2 beamsplitter. A solar tracker with a silicon quadrant sensor centers the solar image on the entrance fieldstop of the FTS. We record the solar intensity at the quadrant sensor at a rate of 0.5 Hz over the 90 s duration of a single-sided scan. The ratio of the standard deviation to the mean of the solar intensity represents the solar intensity variation. If the variation measured by the quadrant sensor for a given interferogram falls below a threshold, we transform the interferogram and retrieve gas columns from the spectrum. Interferograms are recorded on two detectors simultaneously. We obtain full spectral coverage between 3800 and 15750 cm^{-1} using an InGaAs detector (3800-11000 cm^{-1}), and a Si diode detector (10000-15750 cm^{-1}). The detectors are coupled to a 24 bit delta-sigma ADC. We obtain direct solar absorption spectra at 0.02 cm^{-1} resolution (45 cm OPD) and a scan velocity of 10 kHz. For more information on the experimental setup and analysis procedure, see Washenfelder, et al. (2006).[5]

4. Results

Figure 1a shows an interferogram obtained in DC mode on the InGaAs detector. The smoothed, low-pass signal is shown in Figure 1b. This interferogram was obtained with solar intensity variation of 14%; because intensity decreased during the scan, the weight of the high OPD regions of the corrected interferogram, shown in Figure 1c, has been increased, amplifying those fringes and restoring the spectral lines to their correct depths. The re-weighted interferogram is then transformed using slice-ipp, a fast Fourier transform algorithm developed at NASA JPL, which phase corrects the interferogram prior to taking the real-to-complex FFT. We use GFIT, a line-by-line nonlinear least-squares fitting program also developed at NASA JPL to determine atmospheric composition from the spectra.

We test the algorithm by comparing atmospheric column amounts retrieved from spectra derived both from re-weighted interferograms and from control DC interferograms that have not been re-weighted. We use data from both cloudy and clear days to determine the effect of the algorithm on both high quality and potentially compromised data.

Retrievals from the spectra obtained from the re-weighted interferograms show substantially increased precision compared to control data. Shown in Figure 2 are the CO_2 columns retrieved from FTS spectra measured at the US Department of Energy Atmospheric Radiation Measurement site in Darwin, Australia (-12.4 S, 130.9 E) on 29

October 2005. This day was characterized by partly cloudy skies with solar intensity variations between 2% and 50% during individual scans. As the site is coastal, we expect minimal diurnal variability in CO_2. We retrieve near constant gas columns from the re-weighted data over the range of observed solar intensity variation, in contrast to the control data where the scatter in the retrieved columns becomes large at high solar variation. The inset to Figure 2 shows that the re-weighting algorithm reduces the scatter and gives more consistent retrievals even when solar intensity variations fall below 10%. For the full data set of 227 control scans, the column mean is 8.19e21 molecules/cm^2, with a standard deviation of the 227 column values of 6.1e20 molecules/cm^2, or 7%. In contrast, the re-weighted data has a mean column retrieval of 8.25e21 molecules/cm^2, and the standard deviation of the retrievals is 0.6e20 molecules/cm^{2}or 0.7%, an order of magnitude lower. For scans taken with solar intensity variation less than 10%, the standard deviation in the measurements is also reduced by an order of magnitude from 2.5% to 0.25% for the control and re-weighted data, respectively.

To test whether the re-weighting algorithm introduces a bias to the gas retrievals, we use data obtained at Darwin when solar intensity variations were below 3% for all scans recorded. As shown in Figure 3, we see a small negative bias in the re-weighted data. For the 238 scans used from 19 December 2005, the mean difference is -0.016%, with a standard deviation of 0.048% and a standard error of the sampling distribution of 0.003%, indicating a statistically significant negative bias in the re-weighted data.

This bias could be real: the gas columns determined in the control analysis could be higher than the true atmospheric column. We do not have perfect data completely unaffected by SBF on which to test the algorithm, so we must use data with solar intensity variation less than 3% as a proxy. This bias could also be due to artifacts near ZPD in the smoothed interferogram, which will be discussed further in section 6. In either case, the 0.02% bias is quite small and is undetectable in observations made at solar intensity variation between 3-50%. As seen in Figure 3, the difference between the corrected and uncorrected CO_2 column is generally less than 0.1%, with the largest differences at solar intensity variation approaching 3%. The data suggest that the algorithm improves scatter in the retrievals at all solar intensity variations, with its impact on retrievals increasing with solar intensity variation.

Based on the performance of the algorithm in improving retrievals, we have transformed the data obtained at Darwin from August 2005 to August 2006 using the DC re-weighting algorithm. DC acquisition was first implemented in late October 2005, so the first two months of data were obtained in AC mode using a high-pass filter. Figure 4 shows the O_2 volume mixing ratio retrieved at solar intensity variations less than 20%. Note the dramatic transition between the AC and DC regimes. Prior to implementing DC recording, we used a threshold of 2% solar intensity variation to obtain a high precision record under AC acquisition. Using this threshold, we would have discarded all interferograms obtained on 85 out of 286 days between August 2005 and August 2006. Using a higher cutoff of 20% for DC data, the DC re-weighting al-

gorithm has enabled us to include data from those 85 days and improve the quality of the data from the other 201 days.

The signal-to-noise ratio (SNR) of the spectra decreases by approximately 20%, from 840 to 660 near the peak of the InGaAs spectrum and from 390 to 320 near the peak of the Si spectrum, when we switch from AC to DC acquisition. We stress that this reduction in SNR has a negligible effect on our total error budget compared to the errors introduced by uncorrected SBF. The gain of an order of magnitude in precision and the increase to the range of atmospheric conditions in which measurements can be used both far outweigh this 20% reduction in SNR.

5. Non-gray source brightness fluctuations

The theory behind the SBF correction method described here is valid for gray source intensity fluctuations: if the shape of the spectrum remains unchanged, and only its intensity varies, the DC correction should be perfect. However, clouds and aerosol in the atmosphere scatter light preferentially at shorter wavelengths; SBF are thus larger at shorter wavelength than at longer wavelength (ie. non-gray).

To examine the effect of non-gray SBF on our gas retrievals, we distort a sample of ideal interferograms with low relative solar intensity variations (0.5-3%) to simulate the effects of nongray intensity fluctuations. Although the effects of non-gray attenuation could be investigated using a stable light source, we chose instead to model the effects of non-gray SBF as no such lamp was available. We Fourier transform

an ideal interferogram and use $S_{distorted}(\nu) = S_{original}(\nu)\exp(-\tau(\nu/15750)^{\alpha})$ to distort the resulting spectrum for ν between 300 and 15750 cm^{-1}, increasing the value of τ to increase total attenuation (Figure 5a). We choose angstrom exponent, α, of 0.3, a realistic value for clouds in the atmosphere. The ratio of the area under the distorted spectrum to that of the original spectrum between the frequency limits is used to scale the ν=0 point of the distorted DC spectrum and the associated ringing at frequencies below 300 cm^{-1}. The distorted spectra are inverse transformed; the resulting interferograms (Figure 5b) have been influenced by time-independent, non-gray attenuation.

We interpolate between the attenuated interferograms to create an interferogram that exhibits a temporal dependence to the modeled non-gray attenuation (Figure 5c). This interferogram is then re-weighted using the DC correction algorithm (Figure 5d). The control and re-weighted interferograms are transformed (Figure 5 e,f), and gas columns are retrieved from each spectrum. We have simulated two forms of transience: total intensity linearly falling off by 50% at high OPD and total intensity linearly increasing by a factor of 2 from ZPD to maximum OPD.

We retrieve CO_2 and O_2 from two different bands to determine the performance of the DC re-weighting algorithm. The non-gray distortion introduces errors of order 1-4% that are dependent on the characteristics of the fitting window and on the temporal distribution of the distortion. Table 1 shows the impact of these simulations on retrievals from the three bands: CO_2 6180-6260 cm^{-1}, O_2 7765-8005 cm^{-1}, and O_2

12940-13190 cm^{-1} (A-band).

The distorted interferograms that have been re-weighted using our algorithm have errors less than 0.4%, in contrast to errors of several percent in data obtained without using the re-weighting algorithm. These simulations demonstrate that the method is robust to non-gray SBF. In the simulations described in Table 1, we use an angstrom exponent of 0.3 which is a realistic spectral dependence for SBF due to clouds. We further simulated SBF with angstrom exponent as large as 4.0 and still see significant improvements, with errors generally smaller than 0.2% in the column retrievals from re-weighted interferograms. We therefore recommend use of this algorithm for DC-recorded data in all situations, even when the interference exhibits spectral dependence.

6. Artifacts at ZPD

The re-weighting method is sensitive to non-ideal detector behavior near ZPD (Figure 6a). In addition to choosing s in Equation 1 below the low frequency detection limit but above SBF frequency, the filter cutoff can be selected to minimize artifacts resulting from detector nonideality. When using a filter cutoff 80% of our low spectral frequency limit (3000 cm^{-1}), we observed a dip in the low-pass signal at ZPD (Figure 6b). We attribute this dip to detector nonlinearity. Although not discussed further here, this dip can be used to diagnose, model, and account for nonlinearity in the detector. When the frequency cutoff is reduced to 8% of the low frequency limit (300

cm^{-1}), these artifacts are no longer visible, as demonstrated in Figure 6c. The presence of an artifact at ZPD in the smoothed interferograms can bias the resulting fits. The dips at ZPD amplify the center burst of the re-weighted interferogram, raising continuum levels and inducing a negative bias in the retrievals from re-weighted data, an order of magnitude larger than the 0.02% bias observed when s is 8% of the low frequency detection limit. The detector at Darwin exhibits only a small nonlinearity; it is possible that for a detector with a higher degree of nonlinearity, a suitable choice of s above the SBF frequency would not be sufficiently low in frequency to smooth away the artifact observed in Figure 6b. In such a case, the DC correction algorithm would need to be modified to correct for detector non-linearity as well.

7. Conclusion

The influence of SBF on spectra recorded using DC signal processing can be substantially minimized by a simple re-weighting algorithm. We expect this correction method will have an increasingly significant impact on choices made regarding DC versus AC interferogram acquisition, especially as higher resolution ADCs become more prominent in FTS. Even without high resolution ADCs, DC recording of low gain interferograms provides the essential tools for separating the low frequency source variations from high frequency interferometric modulation, enabling source brightness fluctuations to be corrected.

The authors thank David Griffith and Glenn Bryant for their role in data acqui-

sition at the Darwin FTS site. Jean-Francois Blavier is gratefully acknowledged for helpful discussions. This analysis was supported by a grant from NASA (NNGO5-GD07G). The Darwin FTS was developed for the OCO project at NASA JPL; GKA acknowledges support from the NSF Graduate Fellowship Program.

References

1. Ahlers, N.H.E. and H.P. Freedman. "A simple ratio-recording spectrometer", Journal of Scientific Instruments **32**, (1955).
2. Shao, L., M.J. Pollard, P.R. Griffiths, D.T. Westermann, and D.L. Bjorneberg. "Rejection criteria for open-path Fourier transform infrared spectrometry during continuous atmospheric monitoring", Vibrational Spectroscopy **43**, (2007).
3. Brault, J.W. "Fourier Transform Spectrometry" in *High Resolution in Astronomy*, R.S. Booth, J.W. Brault, A. Labeyrie, (Swiss Society of Astrophysics and Astronomy, 1985), pp. 3-62.
4. Kurylo, M.J., and S. Solomon. Network for the Detection of Stratospheric Change, NASA report, Code EEU, Washington, D.C. (1990).
5. Washenfelder, R.W, G.C. Toon, J.-F. Blavier, Z. Yang, N.T. Allen, P.O. Wennberg, S.A. Vay, D.M. Matross, B.C. Daube. "Carbon dioxide column abundances at the Wisconsin Tall Tower site" , J.Geophys.Res **111**, (2006).
6. The Total Carbon Column Observing Network. "http://tccon.caltech.edu".

List of Figure Captions

Fig. 1. (a) Raw DC interferogram with 14% solar intensity variation. (b) Smoothed, low-pass signal. (c) Corresponding re-weighted interferogram.

Fig. 2.A comparison between CO_2 retrievals from re-weighted (dark circles) and the raw control (light squares) spectra as a function of relative solar intensity variation during a 90 s scan. The lower panel zooms in on relative solar intensity variation below 10%.

Fig. 3. The percent difference between CO_2 retrievals from spectra obtained from re-weighted and control interferograms with solar intensity variation less than 3%.

Fig. 4. Time series of the oxygen mixing ratio retrieved from spectra at Darwin, Australia. Prior to November 2005, AC data acquisition was used. Plotted here are data obtained between 20 and 70 degree solar zenith angle. Only spectra obtained with relative solar variation less than 20% are shown.

Fig. 5. A spectrum distorted with non-gray interference of optical depth ranging from 0.0 (original spectrum) to 1.25 at 15750 cm^{-1} (Panel A). The spectra are

inverse Fourier transformed to yield the interferograms in panel B. We interpolate between these interferograms to generate the interferogram in panel C, which exhibits spectrally- and temporally-dependent attenuation compared to the original interferogram. The attenuated interferogram is re-weighted using the DC correction to yield the interferogram in panel D. We then transform each interferogram to yield the control spectrum in panel E, and the re-weighted spectrum in panel F. Although the spectra in E and F appear identical, the line depths in the uncorrected spectrum (E) are more shallow than those in panel F.

Fig. 6. (a) Center burst of raw interferogram. (b) Low pass signal resulting from filter with s = 3000 cm^{-1}. The observed dip at ZPD is likely due to detector nonlinearity. (c) Low pass interferogram resulting from filter with s = 300cm^{-1}. The dip at ZPD has been smoothed away in lowering the frequency cutoff.

Table 1. Retrieval errors [%] from spectra distorted by non-gray SBF.

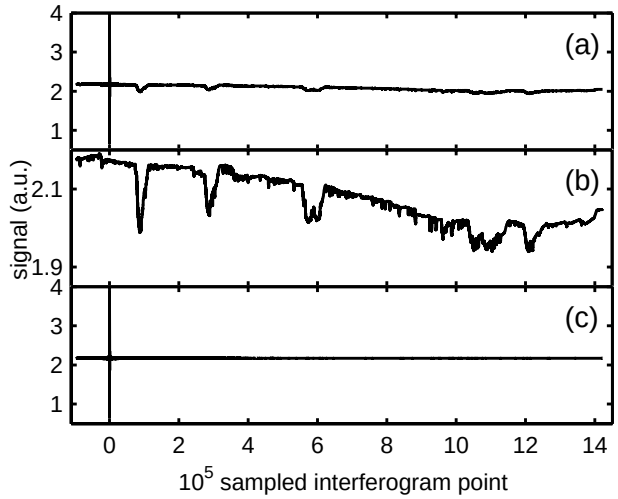

Fig. 1. (a) Raw DC interferogram with 14% solar intensity variation. (b) Smoothed, low-pass signal. (c) Corresponding re-weighted interferogram. igrams3panelAO.eps

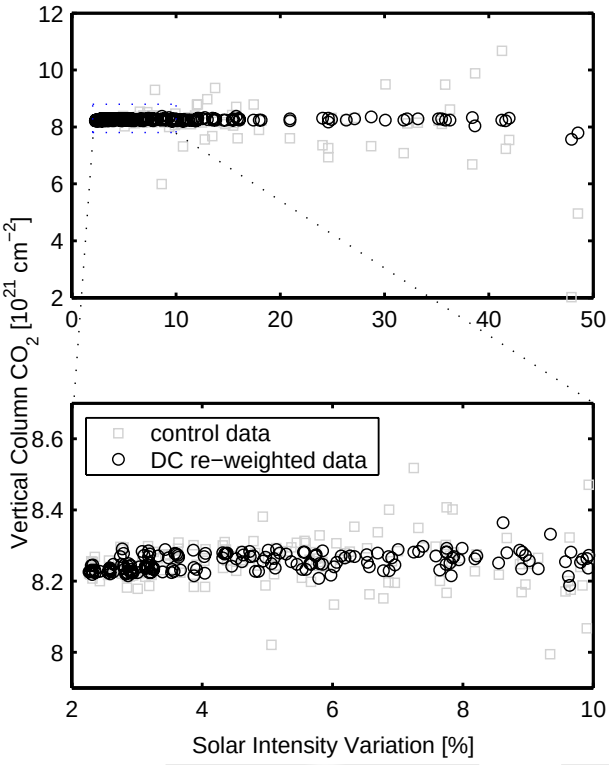

Fig. 2. A comparison between CO_2 retrievals from re-weighted (dark circles) and the raw control (light squares) spectra as a function of relative solar intensity variation during a 90 s scan. The lower panel zooms in on relative solar intensity variation below 10%. cloudyskyAO.eps

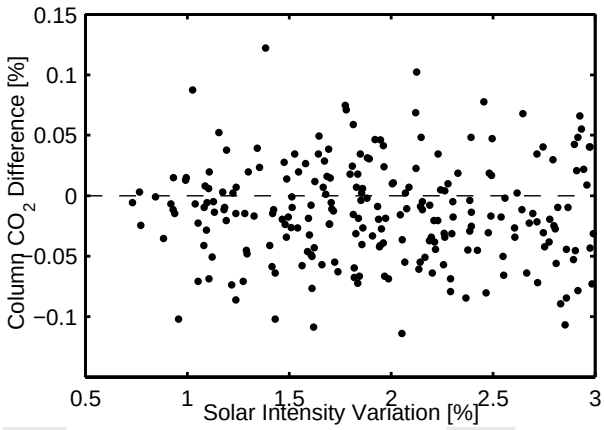

Fig. 3. The percent difference between CO_2 retrievals from spectra obtained from re-weighted and control interferograms with solar intensity variation less than 3%.clearskybiasAO.eps

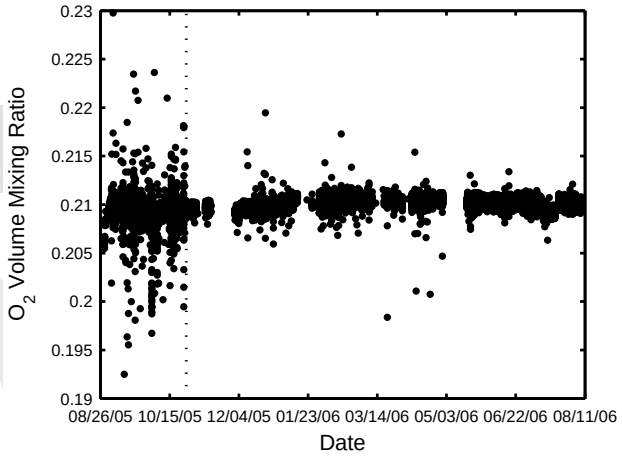

Fig. 4. Time series of the oxygen mixing ratio retrieved from spectra at Darwin, Australia. Prior to November 2005, AC data acquisition was used. Plotted here are data obtained between 20 and 70 degree solar zenith angle. Only spectra obtained with relative solar variation less than 20% are shown. O2timeseriesAO.eps

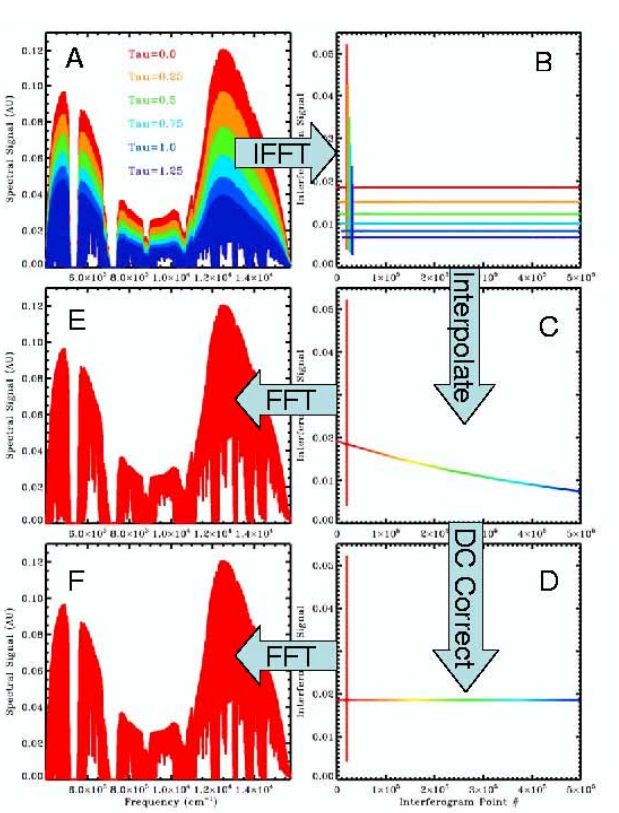

Fig. 5. A spectrum distorted with non-gray interference of optical depth ranging from 0.0 (original spectrum) to 1.25 at 15750 cm^{-1} (Panel A). The spectra are inverse Fourier transformed to yield the interferograms in panel B. We interpolate between these interferograms to generate the interferogram in panel C, which exhibits spectrally- and temporally-dependent attenuation compared to the original interferogram. The attenuated interferogram is re-weighted using the DC correction to yield the interferogram in panel D. We then transform each interferogram to yield the control spectrum in panel E, and the re-weighted spectrum in panel F. Although the spectra in E and F appear identical, the line depths in the uncorrected spectrum (E) are more shallow than those in panel F. nongray3.ps

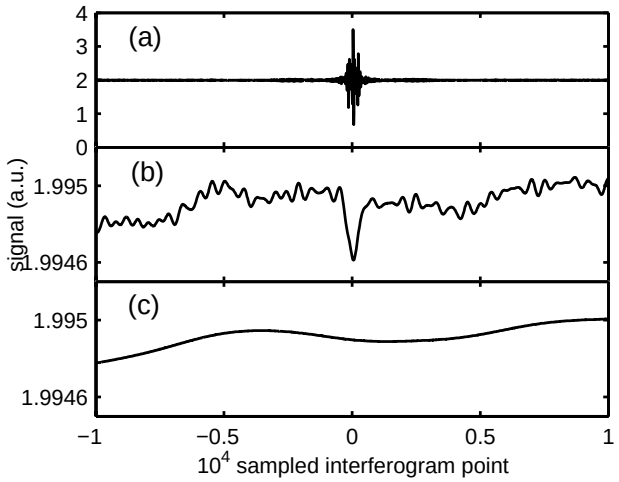

Fig. 6. (a) Center burst of raw interferogram. (b) Low pass signal resulting from filter with s = 3000 cm^{-1}. The observed dip at ZPD is likely due to detector nonlinearity. (c) Low pass interferogram resulting from filter with s = 300cm^{-1}. The dip at ZPD has been smoothed away in lowering the frequency cutoff. zpd3panelAO.eps

Table 1. Retrieval errors [%] from spectra distorted by non-gray SBF.

Retrieved Species	Low OPD Distortion		High OPD Distortion	
	(control)	(re-weighted)	(control)	(re-weighte
CO_2 (6180-6260 cm−1)	4.185	0.081	-1.902	-0.017
O_2 (7765-8005 cm^{-1})	3.264	0.368	-1.442	-0.084
O_2 (12940-13190 cm^{-1})	-0.549	-0.012	0.216	-0.004